THE JOURNAL OF BIOLOGICAL CHEMISTRY VOL. 291, NO. 4, pp. 1751–1762, January 22, 2016

Krüppel Homolog 1 Inhibits Insect Metamorphosis via Direct Transcriptional Repression of *Broad-Complex*, a Pupal Specifier Gene*

Received for publication, September 10, 2015, and in revised form, October 28, 2015 Published, JBC Papers in Press, October 30, 2015, DOI 10.1074/jbc.M115.686121

Takumi Kayukawa[‡1], **Keisuke Nagamine**[‡§], **Yuka Ito**[‡], **Yoshinori Nishita**[¶], **Yukio Ishikawa**[§], **and Tetsuro Shinoda**[‡]

From the [‡]*Insect Growth Regulation Research Unit, National Institute of Agrobiological Sciences, Tsukuba, Ibaraki 305-8634, Japan,* [§]*Laboratory of Applied Entomology, Graduate School of Agricultural and Life Sciences, University of Tokyo, Bunkyo, Tokyo 113–8657, Japan, and* [¶]*Department of Biological Science and Center for Genome Dynamics, Faculty of Science, Hokkaido University, Sapporo, Hokkaido 060-0810, Japan*

The *Broad-Complex* gene (*BR-C*) encodes transcription factors that dictate larval-pupal metamorphosis in insects. The expression of *BR-C* is induced by molting hormone (20-hydroxyecdysone (20E)), and this induction is repressed by juvenile hormone (JH), which exists during the premature larval stage. Krüppel homolog 1 gene (*Kr-h1*) has been known as a JH-early inducible gene responsible for repression of metamorphosis; however, the functional relationship between *Kr-h1* and repression of *BR-C* has remained unclear. To elucidate this relationship, we analyzed *cis*- and *trans* elements involved in the repression of *BR-C* using a *Bombyx mori* cell line. In the cells, as observed in larvae, JH induced the expression of *Kr-h1* and concurrently suppressed 20E-induced expression of *BR-C*. Forced expression of *Kr-h1* repressed the 20E-dependent activation of the *BR-C* promoter in the absence of JH, and *Kr-h1* RNAi inhibited the JH-mediated repression, suggesting that Kr-h1 controlled the repression of *BR-C*. A survey of the upstream sequence of *BR-C* gene revealed a Kr-h1 binding site (KBS) in the *BR-C* promoter. When KBS was deleted from the promoter, the repression of *BR-C* was abolished. Electrophoresis mobility shift demonstrated that two Kr-h1 molecules bound to KBS in the *BR-C* promoter. Based on these results, we conclude that Kr-h1 protein molecules directly bind to the KBS sequence in the *BR-C* promoter and thereby repress 20E-dependent activation of the pupal specifier, *BR-C*. This study has revealed a considerable portion of the picture of JH signaling pathways from the reception of JH to the repression of metamorphosis.

The molting and metamorphosis of insects are intricately regulated by the actions and interactions of ecdysteroids and juvenile hormone (JH).[2] In holometabolous insects, 20-hydroxyecdysone (20E, the primary active ecdysteroid) induces the larval-larval molt in the presence of JH. When the JH titer declines to a trace level in the final larval instar, 20E induces larval-pupal and pupal-adult molts (metamorphosis). Thus, JH plays a key role in preventing larvae from undergoing precocious metamorphosis (1).

Our understanding of the molecular mechanism of JH-mediated repression of insect metamorphosis has significantly advanced (2): JH carried to a target cell is received by a JH receptor, methoprene tolerant (Met) (3–6); JH-liganded Met interacts with steroid receptor coactivator (7–12); the JH/Met/steroid receptor coactivator complex activates Krüppel homolog 1 (*Kr-h1*), a repressor of metamorphosis, by interacting with a JH response element (*k*JHRE) in the *Kr-h1* gene (9, 10, 12–15); Kr-h1 represses the larval-pupal metamorphosis (16–20). To date, however, the mechanism of the repression of metamorphosis by Kr-h1, including target gene(s), binding site(s), and partner(s), has remained unknown.

The Broad-Complex (BR-C) protein is a transcription factor that is composed of a Bric-a-brac/Tramtrack/Broad-Complex (BTB) domain and an alternatively spliced zinc finger domain (Z1-Z6) (21–25). *BR-C* expression is induced by 20E, and BR-C works as a pupal specifier in the larval-pupal transition of holometabolous insects (26–33). In *Manduca sexta* and *Bombyx mori*, removal of the corpora allata (allatectomy), the primary organs for JH synthesis, induced *BR-C* expression and subsequent precocious pupation, and application of exogenous JH to allatectomized larvae inhibited *BR-C* expression and pupation in these larvae (33, 34). JH-mediated repression of the activation of *BR-C* by 20E has been also reported in cultured insect epidermis, but the inhibitory effect of JH declined after the transition to the pupal commitment phase (30, 35). A study using the *Kr-h1* mutant of *Drosophila melanogaster* showed that *Kr-h1* was required for the repression of *BR-C* expression in the fat body of young *D. melanogaster* larvae (36); however, the molecular mechanism underlying the JH-mediated repression of *BR-C*, particularly whether the *BR-C* expression is directly repressed by Kr-h1 or repressed by Kr-h1-inducible gene(s), has remained unclear.

The *BR-C* gene of *B. mori* (*BmBR-C*) has two transcriptional start sites: the distal promoter (P_{dist}) and the proximal promoter (P_{prox}) (37–39). In the *B. mori* cell line BM-N, P_{dist} was activated by 20E, and this activation was repressed by JH, whereas P_{prox} was constitutively activated regardless of the

* This work was supported by JSPS KAKENHI Grant 25850230 (to T. K.). The authors declare that they have no conflicts of interest with the contents of this article.

[1] To whom correspondence should be addressed: Insect Growth Regulation Research Unit, National Institute of Agrobiological Sciences, Ohwashi 1-2, Tsukuba, Ibaraki 305-8634, Japan. Tel.: 81-29-838-6075; Fax: 81-29-838-6075; E-mail: kayu@affrc.go.jp.

[2] The abbreviations used are: JH, juvenile hormone; JHA, juvenile hormone analog; 20E, 20-hydroxyecdysone; BR-C, Broad-Complex; KBS, Kr-h1 binding site; Met, methoprene tolerant.

presence/absence of 20E and JH (Fig. 1*A*) (39, 40). The activation of P_{dist} by 20E was mediated by two ecdysone response elements, one of which interacted with ecdysone receptor/ultraspiracle (Fig. 1*A*) (39, 40).

In the present study we aimed to clarify the molecular mechanism of JH-mediated repression of larval-pupal metamorphosis using a *Bombyx* cell line. Based on the results of the present study, we present a substantive portion of the picture of JH signaling pathways from the reception of JH to the repression of metamorphosis.

Experimental Procedures

Cell Lines—The BM-N cell line, derived from the ovary of *B. mori* (RIKEN BRC), was maintained at 25 °C in IPL-41 medium (Gibco, Invitrogen) containing 10% FBS (HyClone, Logan, UT).

Chemicals—Methoprene (juvenile hormone analog (JHA), SDS Biotech, Tokyo, Japan) was a gift from Dr. Sho Sakurai. 20E was purchased from Sigma.

Construction of Reporter and Expression Plasmids—A reporter plasmid (pGV_$P_{dist_}$−5131/+52) carrying 5′-flanking regions of the distal promoter of *BmBR-C* was prepared as described previously (39, 40). Deleted and mutated reporter plasmids of pGV_P_{dist-}−5131/+52 were constructed by inverse PCR. The primers and templates used for construction of the reporter plasmids are listed in Tables 1 and 2.

An expression plasmid of *BmKr-h1* (pIZT_BmKr-h1) was constructed using the Gateway system (Invitrogen). The full ORF of *BmKr-h1* (AB360766) was amplified by PCR from full-length cDNA clones (9) using the primer containing attB1 and Kozak sequences and the primer containing an attB2 sequence (Table 3). The amplified fragment was inserted into the pDONR 221 plasmid (Invitrogen) and then into the pIZT/V5-His vector (Invitrogen) modified for the Gateway system. The p65AD (from p65, a subunit of NF-κB) (41) was inserted into the N terminus of *BmKr-h1* by inverse PCR using primers shown in Table 3 and a blunt-end ligation kit (Toyobo Co. Ltd., Osaka, Japan). Deleted and mutated pIZT_BmKr-h1 and pIZT_p65AD_BmKr-h1 plasmids were constructed by inverse PCR using primers and templates as shown in Table 3.

For the *in vitro* transcription and translation system, the *BmKr-h1* ORF anchored with SgfI and PmeI sites was amplified by PCR using primers and a template as shown in Table 3. The amplified fragment was digested with Sgf1 and PmeI, and inserted into the pF25A ICE T7 Flexi plasmid (Promega). pF25A plasmids with a C-terminal HA epitope tag (BmKr-h1-HA) and without the C-terminal region downstream of the zinc finger domains (BmKr-h1(1–243)) were constructed by inverse PCR using primers and a template as shown in Table 3.

Double-stranded RNA Synthesis—Template DNA fragments of *BmKr-h1* and *MalE* (control) used for the synthesis of double-stranded RNA were amplified by PCR using primers and templates as shown in Table 4, and PCR products were purified using a Wizard SV Gel and PCR Clean-Up System (Promega). Double-stranded RNAs were synthesized from the amplified DNA using RiboMAX SP6 and T7 Large Scale RNA Production Systems according to the manufacturer's instructions (Promega).

Transfection and Reporter Assays—BM-N cells were seeded at a density of 1.5×10^5 cells/well in 200 μl medium in a 96-well plate (Sumilon, Sumilomo Bakelite Co., Tokyo, Japan) 1 day before transfection. Transfection of BM-N cells was performed using FuGENE HD (Promega, Madison, WI). The pIZT_RLuc vector containing the *Renilla* luciferase gene was constructed as the reference for BM-N cells (42). The cells were incubated for 1 day (Fig. 1*B*) or 2 days (Figs. 2, *B, C* and *D*, 3*A*, and 6*A*) after transfection and treated with JHA or 20E for 2 days. The treated cells were then processed by using the Dual-Luciferase reporter assay system (Promega) according to the manufacturer's instructions and analyzed with a luminometer (ARVO, PerkinElmer Life Sciences).

Quantitative Real-time PCR—Total RNA was extracted from BM-N cells using an RNeasy Plus mini kit (Qiagen, Venlo, The Netherlands) and used to synthesize cDNAs with a PrimeScript RT reagent kit (TaKaRa Bio, Ohtsu, Japan). To examine the time course of *BmKr-h1* expression after JHA treatment, the primers designed to amplify both isoforms of *BmKr-h1* have been described previously (9). For evaluation of the efficiency of RNAi, the primers designed to amplify both isoforms of *BmKr-h1* were shown in Table 4. *BmRp49* was used as the internal reference (9). The reaction was carried out in a 10-μl reaction volume containing template cDNA derived from 1 ng of total RNA, SYBR Premix Ex Taq (TaKaRa Bio), and 0.2 μM concentrations of each primer using a LightCycler 480 real-time thermal cycler (Roche Applied Science). The PCR conditions were 95 °C for 5 min and 55 cycles of 95 °C for 5 s and 60 °C for 20 s. The relative amounts of the transcripts were calculated by a crossing point analysis using standard curves generated from a plasmid containing a fragment of each gene. The expression levels of *BmKr-h1* were normalized by those of *BmRp49*, and the levels of *BmKr-h1* transcript at 2 h after JHA treatment (Fig. 2*A*) and of *dsMalE* after 20E and JHA treatment (Fig. 2*C*) were set as 100.

Electrophoresis Mobility Shift Assay (EMSA)—EMSA was performed using the LightShift Chemiluminescent EMSA Kit (Pierce). Oligonucleotides labeled with 5′-terminal Biotin-ON were purchased from Eurofins Genomics (Tokyo, Japan); the sequences are shown in Table 4. The oligonucleotide pairs were mixed together, heated at 95 °C for 5 min, and annealed at room temperature for 1.5 h. The resultant double-stranded DNA was used as a probe for EMSA. Specific and nonspecific competitors (Table 4) were also prepared by the method described above. The *in vitro* transcription and translation of BmKr-h1-HA, BmKr-h1(1–243), and Luciferase (mock) were performed with the TNT T7 Insect Cell Extract Protein Expression System (Promega). Binding reactions were carried out in a 10-μl volume containing 0.02 pmol probe, 1.5 μl TNT reaction, 10 × Binding Buffer (Pierce), 0.5 μg of poly (dI-dC), 2.5% glycerol, 0.05% Nonidet P-40, 10 mM KCl, 1 mM $MgCl_2$, 1 mM $ZnSO_4$, and 2 mM EDTA at 25 °C for 2 or 4 h. In competition and antibody assays, the reaction mixture was incubated with 100-fold (2 pmol) unlabeled competitors and 1 μl of tag antibody (Abcam, Cambridge, UK), respectively. The samples were then electrophoresed at room temperature on a 4% nondenaturing polyacryl-

TABLE 1
List of primers and templates used for construction of reporter plasmids

Name	Figure	PCR template	Nucleotide sequence (5′ to 3′)
pGV_$P_{dist_}$−5131/+52[a]	Figs. 1*B*; 2, *B* and *D*; 3, *A*, *B*, and *D*; 5, *A* and *B*; 6*A*		
pGV_$P_{dist_}$−5131/+52_ΔE-box(−4362/−4357)	Fig. 1*B*	pGV_$P_{dist_}$−5131/+52	AAAATCGTTTTTTTCTGTTATTTATTTGTTTGTTTGTTATTTAGTTTTTTGTG TTTTGAACGATTCAATTCTAAATTCTAAGCGCTACG
pGV_$P_{dist_}$−5131/+52_ΔE-box(-1066/-1061)	Fig. 1*B*	pGV_$P_{dist_}$−5131/+52	AAAAAATGAAAATTAGGTTATATTTTTATGACTCTTTTTTCAAAATTCAAC TTTATTCGTTCTAAAGCTATTTCATTTCATTGAATTGAGACATG
pGV_$P_{dist_}$−5131/−3008 and −511/+52	Fig. 3, *B* and *C*	pGV_$P_{dist_}$−5131/+52	GAAAACACTTTTCGGAACTTTCACTTCATTGG CTAACAACAAAATGGATTGCTCTACCCATATAC
pGV_$P_{dist_}$−4609/−3008 and −511/+52	Fig. 3, *B*, *C*, *F*, and *G*	pGV_$P_{dist_}$ − 5131/ − 3008 and − 511/+52	GCTCTCTGTTTATCATGGGTCAATAAAGAAGTC GAGCTCGGTACCTCCCGGGTTATG
pGV_$P_{dist_}$−5131/−4714 and −4086/−3008 and −511/+52	Fig. 3*B*	pGV_$P_{dist_}$ − 5131/ − 3008 and − 511/+52	GAATGGTGGTAAATATCTTCTCTCTCAATGTAGTTAAG CAGATTGCGGATATACACGTTTCGTCATTGAG
pGV_$P_{dist_}$−5131/-4199 and −3575/−3008 and −511/+52	Fig. 3*B*	pGV_$P_{dist_}$ − 5131/ − 3008 and − 511/+52	CCATTAAACATTTCCATAAAAACCTACGAATGTGAATTAAC GGCCTTGGAATTAATTCTGTACTTCAATCATG
pGV_$P_{dist_}$−4469/−3008 and −511/+52	Fig. 3*C*	pGV_$P_{dist_}$ − 5131/ − 3008 and − 511/+52	ACGTCTATCCGTGACCTACGCTAACG GAGCTCGGTACCTCCCGGGTTATG
pGV_$P_{dist_}$-4449/−3008 and −511/+52	Fig. 3*C*	pGV_$P_{dist_}$ − 5131/ − 3008 and − 511/+52	CTAACGCTAAATAGAGTTCCGACCTTGACTC GAGCTCGGTACCTCCCGGGTTATG
pGV_$P_{dist_}$-4429/−3008 and −511/+52	Fig. 3*C*	pGV_$P_{dist_}$ − 5131/ − 3008 and − 511/+52	GACCTTGACTCTAACGGTCGTCGAC GAGCTCGGTACCTCCCGGGTTATG
pGV_$P_{dist_}$−4609/−4410 and −511/+52	Fig. 3*C*	pGV_$P_{dist_}$ − 4609/ − 3008 and − 511/+52	GAAAACACTTTTCGGAACTTTCACTTCATTGG CGACCGTTAGAGTCAAGGTCGGAAC
pGV_$P_{dist_}$−4609/−4430 and −511/+52	Fig. 3*C*	pGV_$P_{dist_}$ − 4609/ − 3008 and − 511/+52	GAAAACACTTTTCGGAACTTTCACTTCATTGG GGAACTCTATTTAGCGTTAGCGTAGGTCAC
pGV_$P_{dist_}$−4609/−4450 and −511/+52	Fig. 3*C*	pGV_$P_{dist_}$ − 4609/ − 3008 and − 511/+52	GAAAACACTTTTCGGAACTTTCACTTCATTGG CGTAGGTCACGGATAGACGTAGAGC
pGV_$P_{dist_}$−5131/+52_ΔKBS	Fig. 2*D*, 6*A*	pGV_$P_{dist_}$−5131/+52	TCGACTCTACATTACGTAGCGCTTAGAATTTAG AGAGCGCACAAATAAATTTCATGATCTTTATTAAAAACAC
pGV_$P_{dist_}$ KBS and −511/+52	Fig. 2*D*	pGV_$P_{dist_}$ − 4469/ − 3008 and − 511/+52	GAAAACACTTTTCGGAACTTTCACTTCATTGG CGACCGTTAGAGTCAAGGTCGGAAC
pGV_$P_{dist_}$−511/+52	Fig. 2*D*	pGV_$P_{dist_}$ − 5131/ − 3008 and − 511/+52	GAAAACACTTTTCGGAACTTTCACTTCATTGG GAGCTCGGTACCTCCCGGGTTATG
pGV_$P_{dist_}$-1537/+52	Fig. 1*A*	pGV_$P_{dist_}$−5131/+52	CATTGCTTTCGTCCGGTGACATCTTATTAG GAGCTCGGTACCTCCCGGGTTATG

[a] See Nishita and Takiya (40).

TABLE 2
List of primers, methods, and templates used for construction of reporter plasmids with transversion and transition

Name	Figure	PCR template	Nucleotide sequence (5′ to 3′)
pGV_$P_{dist_}$−4609/−3008 and −511/+52_TV1	Fig. 3*F*	pGV_$P_{dist_}$ − 5131/ − 3008 and − 511/+52	GAGATCCGTGACCTACGCTAACGCTAAATAGAG ATGAGAGCGCACAAATAAATTTCATGATCTTTATTAAAAACAC
pGV_$P_{dist_}$−4609/−3008 and −511/+52_TV2	Fig. 3*F*	pGV_$P_{dist_}$ − 5131/ − 3008 and − 511/+52	ATGGACCTACGCTAACGCTAAATAGAGTTCCG TCGAGACGTAGAGCGCACAAATAAATTTCATGATC
pGV_$P_{dist_}$−4609/−3008 and −511/+52_TV3	Fig. 3*F*	pGV_$P_{dist_}$ − 5131/ − 3008 and − 511/+52	AGCCGCTAACGCTAAATAGAGTTCCGACCTTG TGAACGGATAGACGTAGAGCGCACAAATAAATTTC
pGV_$P_{dist_}$−4609/−3008 and −511/+52_TV4	Fig. 3*F*	pGV_$P_{dist_}$ − 5131/ − 3008 and − 511/+52	GCCCGCTAAATAGAGTTCCGACCTTGACTCTAAC TATTAGGTCACGGATAGACGTAGAGCGC
pGV_$P_{dist_}$−4609/−3008 and −511/+52_TV5	Fig. 3*F*	pGV_$P_{dist_}$ − 5131/ − 3008 and − 511/+52	GCCATAGAGTTCCGACCTTGACTCTAACGGTC TATTTAGCGTAGGTCACGGATAGACGTAGAG
pGV_$P_{dist_}$−4609/−3008 and −511/+52_TV6	Fig. 3*F*	pGV_$P_{dist_}$ − 5131/ − 3008 and − 511/+52	TCTTTCCGACCTTGACTCTAACGGTCGTC GCGTTAGCGTTAGCGTAGGTCACGGATAGAC
pGV_$P_{dist_}$−4609/−3008 and −511/+52_TV7	Fig. 3*F*	pGV_$P_{dist_}$ − 5131/ − 3008 and − 511/+52	ATCCCTTGACTCTAACGGTCGTCGACTC TCCCTCTATTTAGCGTTAGCGTAGGTCACGG
pGV_$P_{dist_}$−4609/−3008 and −511/+52_TV8	Fig. 3*F*	pGV_$P_{dist_}$ − 5131/ − 3008 and − 511/+52	GTCCTCTAACGGTCGTCGACTCTACATTACG CTTTCGGAACTCTATTTAGCGTTAGCGTAGGTC
pGV_$P_{dist_}$−4609/−3008 and −511/+52_TV9	Fig. 3*F*	pGV_$P_{dist_}$ − 5131/ − 3008 and − 511/+52	GCCCGGTCGTCGACTCTACATTACGTAGC TCTTCAAGGTCGGAACTCTATTTAGCGTTAGC
pGV_$P_{dist_}$−4609/−3008 and −511/+52_TV10	Fig. 3*F*	pGV_$P_{dist_}$ − 5131/ − 3008 and − 511/+52	GATTCGACTCTACATTACGTAGCGCTTAGAATTTAG AATTTAGAGTCAAGGTCGGAACTCTATTTAGCG
pGV_$P_{dist_}$−4609/−3008 and −511/+52_TS1	Fig. 3*G*	pGV_$P_{dist_}$ − 5131/ − 3008 and − 511/+52	CTCATCCGTGACCTACGCTAACGCTAAATAGAG TACAGAGCGCACAAATAAATTTCATGATCTTTATTAAAAACAC
pGV_$P_{dist_}$−4609/−3008 and −511/+52_TS2	Fig. 3*G*	pGV_$P_{dist_}$ − 5131/ − 3008 and − 511/+52	TACGACCTACGCTAACGCTAAATAGAGTTCCG AGCAGACGTAGAGCGCACAAATAAATTTCATGATC
pGV_$P_{dist_}$−4609/−3008 and −511/+52_TS3	Fig. 3*G*	pGV_$P_{dist_}$ − 5131/ − 3008 and − 511/+52	TCGCGCTAACGCTAAATAGAGTTCCGACCTTG ACTACGGATAGACGTAGAGCGCACAAATAAATTTC
pGV_$P_{dist_}$−4609/−3008 and −511/+52_TS4	Fig. 3*G*	pGV_$P_{dist_}$ − 5131/ − 3008 and − 511/+52	CGGCGCTAAATAGAGTTCCGACCTTGACTCTAAC ATATAGGTCACGGATAGACGTAGAGCGC
pGV_$P_{dist_}$−4609/−3008 and −511/+52_TS5	Fig. 3*G*	pGV_$P_{dist_}$ − 5131/ − 3008 and − 511/+52	CGGATAGAGTTCCGACCTTGACTCTAACGGTC ATATTAGCGTAGGTCACGGATAGACGTAGAG
pGV_$P_{dist_}$−4609/−3008 and −511/+52_TS6	Fig. 3*G*	pGV_$P_{dist_}$ − 5131/ − 3008 and − 511/+52	AGATTCCGACCTTGACTCTAACGGTCGTC CGCTTAGCGTTAGCGTAGGTCACGGATAGAC
pGV_$P_{dist_}$−4609/−3008 and −511/+52_TS7	Fig. 3*G*	pGV_$P_{dist_}$ − 5131/ − 3008 and − 511/+52	TAGCCTTGACTCTAACGGTCGTCGACTC AGGCTCTATTTAGCGTTAGCGTAGGTCACGG
pGV_$P_{dist_}$−4609/−3008 and −511/+52_TS8	Fig. 3*G*	pGV_$P_{dist_}$ − 5131/ − 3008 and − 511/+52	CAGCTCTAACGGTCGTCGACTCTACATTACG GAATCGGAACTCTATTTAGCGTTAGCGTAGGTC
pGV_$P_{dist_}$−4609/−3008 and −511/+52_TS9	Fig. 3*G*	pGV_$P_{dist_}$ − 5131/ − 3008 and − 511/+52	CGGCGGTCGTCGACTCTACATTACGTAGC AGATCAAGGTCGGAACTCTATTTAGCGTTAGC
pGV_$P_{dist_}$−4609/−3008 and −511/+52_TS10	Fig. 3*G*	pGV_$P_{dist_}$ − 5131/ − 3008 and − 511/+52	CTATCGACTCTACATTACGTAGCGCTTAGAATTTAG TTATTAGAGTCAAGGTCGGAACTCTATTTAGCG

TABLE 3
List of primers used for construction of expression plasmids

Name	Figure	PCR template	Nucleotide sequence (5′ to 3′)
pIZT_BmKr-h1	Fig. 2*B*, 3*A*, and 6*A*	Full length cDNA clone	AAAAAGCAGGCTTCGAAGGAGATAGAACCATGATAGGTGACGAGGAGCGAG AGAAAGCTGGGTCCTATGATTCTGTAGCTGGCGGAG
pIZT_p65AD_BmKr-h1	Figs. 3, *A*, *B*, *C*, *D*, *F*, and *G*; 5, *A* and *B*	pIZT_BmKr-h1	ATGATAGGTGACGAGGAGCGAGTTCATC GGTTCTATCTCCTTCGAAGCCTGCTTTTTT ATGTTCCCTTCTGGGCAAATCTCAAACCAGG TTGGCCGCTGGAGCTGATCTGACTC
pIZT_p65AD		pIZT_p65AD_BmKr-h1	ACCCAGCTTTCTTGTACAAAGTGGTCCC CTATTGGCCGCTGGAGCTGATCTGACTC
pF25A_BmKr-h1		pIZT_BmKr-h1	TTTGCGATCGCATGATAGGTGACGAGGAGCGAG TTTGTTTAAACCTATGATTCTGTAGCTGGCGGAGCAAATTG
pF25A_BmKr-h1_HA	Fig. 4, *A* and *B*	pF25A_BmKr-h1	TCCCGGACTATGCAGGATCCTATCCATATGACGTTCCAGATTACGCTTGAGTTTAAAC GAATTCGGGCTCGGTACCC CGTCATAGGGATAGCCCGCATAGTCAGGAACATCGTATGGGTATGATTCTGTAGCTG GCGGAGCAAATTGTATAAC
pF25A_BmKr-h1(1–243)	Fig. 4*B*	pF25A_BmKr-h1	TGAGTTTAAACGAATTCGGGCTCGGTACCC ACTCTGTAATGGTGCGGTGCGGGG
pIZT_p65AD_BmKr-h1_ΔZF1	Fig. 5*A*	pIZT_p65AD_BmKr-h1	CGTTCTACTGCTGATGCACATCGCTGC CTGATGAACTCGCTCCTCGTCACCTATC
pIZT_p65AD_BmKr-h1_ΔZF2	Fig. 5*A*	pIZT_p65AD_BmKr-h1	ACTGGCGAGCGACCATTTGAATGTGAATATTG GCGATGTGCATCAGCAGTAGAACGATG
pIZT_p65AD_BmKr-h1_ΔZF3	Fig. 5*A*	pIZT_p65AD_BmKr-h1	ACAAAGGAGAGGCCGTATCGGTGCAATG TTCAAATGGTCGCTCGCCAGTATGGGTTC
pIZT_p65AD_BmKr-h1_ΔZF4	Fig. 5*A*	pIZT_p65AD_BmKr-h1	ACCGGCGAGAGACCGCACGCATG CCGATACGGCCTCTCCTTTGTGTGAATAC
pIZT_p65AD_BmKr-h1_ΔZF5	Fig. 5*A*	pIZT_p65AD_BmKr-h1	ACAGGTGAGAAACCCTATCGTTGTCCTG TGCGTGCGGTCTCTCGCCGGTAT
pIZT_p65AD_BmKr-h1_ΔZF6	Fig. 5*A*	pIZT_p65AD_BmKr-h1	ACGGGAGAGCGACCCTATACTTGTG ACGATAGGGTTTCTCACCTGTGTGGG
pIZT_p65AD_BmKr-h1_ΔZF7	Fig. 5*A*	pIZT_p65AD_BmKr-h1	TTTGGCGAGCGCTGTTATCGTTGCACTG AGTATAGGGTCGCTCTCCCGTGTGAG
pIZT_p65AD_BmKr-h1_ΔZF8	Fig. 5*A*	pIZT_p65AD_BmKr-h1	GGCGCGGAAGCCCCCCGCA GCGCTCGCCAAAATGTTGAAAACGATGTAAT
pIZT_p65AD_BmKr-h1_ZF1_amino acid substitution	Fig. 5*B*	pIZT_p65AD_BmKr-h1	GCAGTGCGCTTACAGCATTCGCACGATCCTTTCGTTC GGGTGGACAATGTCAAACCAGACTCGCCGGACTGAT
pIZT_p65AD_BmKr-h1_ZF2_amino acid substitution	Fig. 5*B*	pIZT_p65AD_BmKr-h1	CTGCACGACTCGTGCGCTTCTACCGAACCTTTACTGG GCACAGCAAAAGTCTTATGGGACACGTCGGAGCGAT
pIZT_p65AD_BmKr-h1_ZF3_amino acid substitution	Fig. 5*B*	pIZT_p65AD_BmKr-h1	AAGAAAATTTGCAAGTATTCCGTCGTATTTTCACAAA TCACACTAAACATTTTATGGGAATATTCAGATTCAA
pIZT_p65AD_BmKr-h1_ZF4_amino acid substitution	Fig. 5*B*	pIZT_p65AD_BmKr-h1	CCGGAAAACTTCACAGATTTGCTAGAATCTTTACCGG AATGCTCGAATGCCGCATCAGAAACATTGGACCGAT
pIZT_p65AD_BmKr-h1_ZF5_amino acid substitution	Fig. 5*B*	pIZT_p65AD_BmKr-h1	CTGGTCAACTGGTCATATTTTTAAGGACCTTCACAGG ATTGTATGAACGTCTTATGAGAATGTGGAGATGCGT
pIZT_p65AD_BmKr-h1_ZF6_amino acid substitution	Fig. 5*B*	pIZT_p65AD_BmKr-h1	TCCTCTAAACAGCTTAAAGTATTTTCTCGTACTTTCACGGG GGTGAAGCCCTTTCCGGATCCAGGTGCAGGAGAACGAT
pIZT_p65AD_BmKr-h1_ZF7_amino acid substitution	Fig. 5*B*	pIZT_p65AD_BmKr-h1	ATCATGTTCTCAAATTATTTCGTTTTCAATTTTTTGG TATAACCAAAGTCCCTGAGAGAAATTTCAGAAGTAT
pIZT_p65AD_BmKr-h1_ZF8_amino acid substitution	Fig. 5*B*	pIZT_p65AD_BmKr-h1	CAAAAAAACAAATGGAAGCCTTTATTTACAAAGAATTTGGCGC

TABLE 4
List of primers and oligonucleotides used for dsRNA syntheses and EMSA
q-PCR, quantitative real-time PCR.

Name	Figure	PCR template	Nucleotide sequence (5′ to 3′)
dsRNA			
dsMalE	Fig. 2, *C* and *D*	pMAL-c4E (NEB)	GGATCCTAATACGACTCACTATAGGTGATTGCTGCTGACGGGGGT
			GGATCCTAATACGACTCACTATAGGTTTCTGGGCGTTTTCCATAGTGG
dsBmKr-h1	Fig. 2, *C* and *D*	pIZT_BmKr-h1	GGATCCTAATACGACTCACTATAGGATGATAGGTGACGAGGAGCGAG
			GGATCCTAATACGACTCACTATAGGGCTCTCCCGTGTGAGTACGAG
qPCR			
BmKr-h1_RNAi_qPCR	Fig. 2*C*	cDNA	CATCGTTTTCAACATTTTGGCGAG
			CACATCACTTTTACCATCGGCAGC
EMSA			
Probe (−4480/−4401)	Fig. 4, *A* and *B*		Biotin-ON-tgtgcgcttACGTCTATCCGTGACCTACGCTAACGCTAAATAGAGTTCCGACCTTGACTCTAACGGTCGtcgacttctac
			Biotin-ON-gtagagtcgaCGACCGTTAGAGTCAAGGTCGGAACTCTATTTAGCGTTAGGTCACGGATAGACGTagagcgcaca
Specific competitor (−4480/−4401)	Fig. 4, *A* and *B*		tgtgcgcttACGTCTATCCGTGACCTACGCTAACGCTAAATAGAGTTCCGACCTTGACTCTAACGGTCGtcgacttctac
			gtagagtcgaCGACCGTTAGAGTCAAGGTCGGAACTCTATTTAGCGTTAGGTCACGGATAGACGTagagcgcaca
Non-specific competitor (−4054/−3975)	Fig. 4, *A* and *B*		TTAAGAAGTTTCACTTCCGATTTGTTTATTAAACTAATCAAGTTGTTTCATTCTGAAATATTATTATTTGAGACTA
			TAGTCTCTCAAATAATAATATTTCAGAATGAAAACAACTTGATTAGTTTTAATAAAACAAATCGGAAGTGAAACTTCTTAA

amide gel in 0.5 × Tris borate-EDTA. The probes in electrophoresed gels were transferred to positively charged nylon membranes (Roche Applied Science) by electrophoresis. The nylon membranes were then processed using the LightShift Chemiluminescent EMSA kit according to the manufacturer's instructions and detected with a LAS-3000 mini (Fujifilm, Tokyo, Japan).

Results and Discussion

Hormonal Regulation via E-box Sequences of the BR-C Promoter—In BM-N cells, a reporter carrying the upstream region (−5131 to +52; KAIKObase) of *BmBR-C*_P_{dist} was activated by 20E, and this activation was repressed by a JH analog methoprene (JHA) (Fig. 1*B*) in accordance with previous studies (39, 40). In general, bHLH-PAS transcription factors, to which Met belongs, recognize DNA sequences with a hexanucleotide core known as the E-box (CANNTG) (43). The core sequence of *k*JHRE has been identified as a 12-bp sequence that contains a palindromic canonical E-box (CACGTG), with which two Met paralogs of *B. mori* (BmMet1 and BmMet2) interact (9, 12). We found two CACGTG E-box sequences in the upstream sequence of *BmBR-C*_P_{dist}, *i.e.* positions −4362 to −4357 and −1066 to −1061 (Fig. 1*B*). We carried out reporter assays using constructs mutated in the E-box sequences to examine whether these sequences contribute to the JH-mediated repression of the activation of *BmBR-C*_P_{dist}. The reporter activities observed in response to 20E and JHA were only minimally affected by the mutation of either of the two E-box sequences (Fig. 1*B*), indicating that the contribution of the two E-box sequences to the JH-mediated repression was negligible.

Repression of the BR-C Promoter by BmKr-h1—Kr-h1 has been reported to be induced by JH in several insects *in vivo* and also in several insect cell lines (8–10, 16–20). In BM-N cells, the ordinary expression level of *BmKr-h1* transcripts was marginal, but it increased 37-, 254-, and 1025-fold by 0.5, 1, and 2 h after JHA treatment, respectively (Fig. 2*A*). To examine the involvement of BmKr-h1 in the JH-mediated repression against the activation of *BmBR-C*_P_{dist} by 20E, we carried out reporter assays using BM-N cells. Ectopic expression of BmKr-h1 repressed the activation of a reporter carrying the −5131 to +52 region of *BmBR-C*_P_{dist} (Fig. 2*B*). We next performed reporter assays in BM-N cells in combination with RNAi. In cells treated with *dsBmKr-h1*, the levels of *BmKr-h1* transcripts observed following 20E and JHA treatments declined to about one-third that of those in the cells untreated with double-stranded RNA, whereas treatment with *dsMalE* (control) showed no effects on *BmKr-h1* transcript levels (Fig. 2*C*). RNAi silencing of *BmKr-h1* alleviated the repression of the reporter activities by JHA (Fig. 2*D*), reconfirming that BmKr-h1 repressed the activation of *BmBR-C*_P_{dist}.

Identification of KBS in the BR-C Promoter—Insect Kr-h1 proteins commonly have eight C_2H_2 zinc finger domains, which putatively bind to a specific DNA sequence (9, 17). We hypothesized that BmKr-h1 directly binds to the *BmBR-C*_P_{dist} region and represses the activation of *BmBR-C*_P_{dist} by 20E. To identify a putative BmKr-h1 binding sequence, we employed a

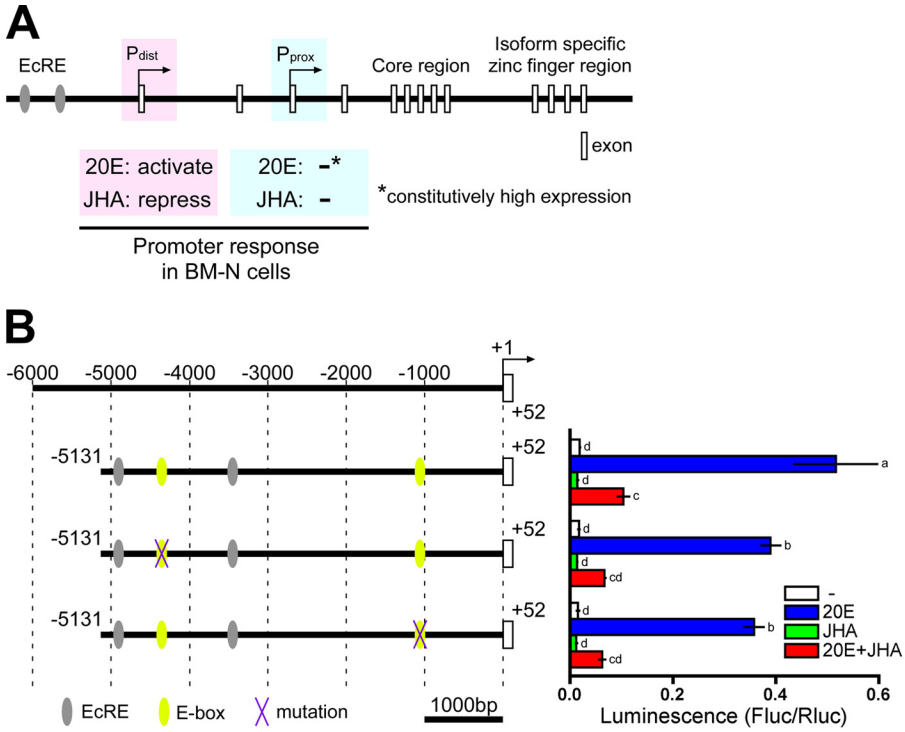

FIGURE 1. **Genomic structure of *BmBR-C*, hormonal responses of its promoter with reference to its E-box sequences.** *A*, schematic representation of the genomic structure of *BmBR-C*. Predicted exons are shown as *boxes*. The *BmBR-C* gene has two transcriptional start sites (the distal promoter (P_{dist}) and the proximal promoter (P_{prox})). In BM-N cells, P_{dist} was activated by 20E via two ecdysone response elements (*EcRE*; *gray ellipses*), and the activation was repressed by JHA, whereas the P_{prox} transcript was constitutively highly expressed regardless of 20E and methoprene (JHA) (40). *B*, functional characterization of the E-box sequences in *BmBR-C*_P_{dist}. *Yellow ellipses* indicate two E-box sequences (−4362 to −4357 and −1066 to −1061) located in the upstream region of *BmBR-C*_P_{dist} (−5131 to +52). *Purple X* marks indicate mutations of E-box sequence. BM-N cells were cotransfected with reporter plasmids that express firefly luciferase (*Fluc*) under the regulation of the regions indicated in the figure (−5131 to +52) and a reference reporter plasmid carrying *Renilla* luciferase (*Rluc*). Cells were treated with 1 μM 20E and/or 10 μM methoprene (JHA) for 2 days. Reporter activities were measured using a dual-luciferase reporter assay system. Data represent the means ± S.D. (n = 3). *Bars* with the same letter are not significantly different (Tukey-Kramer test, α = 0.05).

p65AD_BmKr-h1 expression vector in which BmKr-h1 was fused with the activation domain of p65 (p65AD), a subunit of NF-κB (41). Through this modification, if p65AD_BmKr-h1 bound to the *BmBR-C*_P_{dist} region, the luciferase reporter downstream of the *BmBR-C*_P_{dist} region would be forcibly activated by p65AD. We first confirmed that overexpression of p65AD alone did not affect the reporter activities (data not shown). Then, we tested a construct carrying the upstream region (−5131 to +52) of *BmBR-C*_P_{dist}. Although the activation of this reporter by 20E was repressed by the overexpression of native BmKr-h1 (Fig. 2*B* and Fig. 3*A*), p65AD-BmKr-h1 consistently activated the reporter regardless of the presence of 20E or 20E/JHA (Fig. 3*A*). Because the activity of the reporter carrying the region −1537 to +52 was not increased by p65AD-BmKr-h1, the binding site of BmKr-h1 was considered to lie between −5131 and −1537 (Fig. 3*A*). Next, we tested the reporter activities of several deletion constructs (−5131 to −3008, −4609to −3008, −5131 to −4714/−4086 to −3008, and −5131 to −4199/−3575 to 3008; Fig. 3*B*). All constructs except the ones carrying the regions −5131 to −4714/−4086 to −3008 showed an increase in luciferase reporter activity in the presence of p65AD-BmKr-h1, suggesting that the binding site of BmKr-h1 lay between −4609 and −4199. Subsequent reporter assays of constructs from which 20-bp fragments were serially deleted from both sides of the sequence −4609to −4199 revealed that the crucial region for the response to JH was −4469 to −4410 (Fig. 3*C*). This 60-bp region of Kr-h1 binding was referred to as KBS.

To confirm the identification of KBS, we constructed two reporters, one carrying the −5131 to +52 region without KBS and the other carrying the KBS region connected with the basal promoter region (−511 to +52) (Fig. 3*D*). The deletion of KBS resulted in a disappearance of reporter activity induced by p65AD-BmKr-h1, whereas the reporter carrying KBS and the basal promoter was sufficient for activation by p65AD-BmKr-h1 (Fig. 3*D*), indicating that KBS included the target sequence for BmKr-h1. Interestingly, KBS was located between the two ecdysone response elements of *BmBR-C*_P_{dist} (Fig. 3*E*).

To pinpoint sequences within KBS that are indispensable for the binding of BmKr-h1, transversion (A ↔ C and T ↔ G) and transition (A ↔ G and T ↔ C) mutations were introduced. Reporter activity was drastically reduced when a mutation was introduced into $^{-4457}$GACCTA, $^{-4451}$CGCTAA (Fig. 3*F*), $^{-4439}$ATAGAG, or $^{-4433}$TTCCGA (Fig. 3*G*). These results indicated that the 30-bp sequence encompassing −4457 to −4428 (GACCTACGCTAACGCTAAATAGAGTTCCGA) is crucial for the binding of BmKr-h1 (Fig. 3*E*, *pink highlight*). We referred to the sequence as the KBS core region. Although Krüppel, a gap gene of *D. melanogaster* involved in the development of segmented embryos, has four zinc finger domains similar to those of Kr-h1, the binding consensus sequence

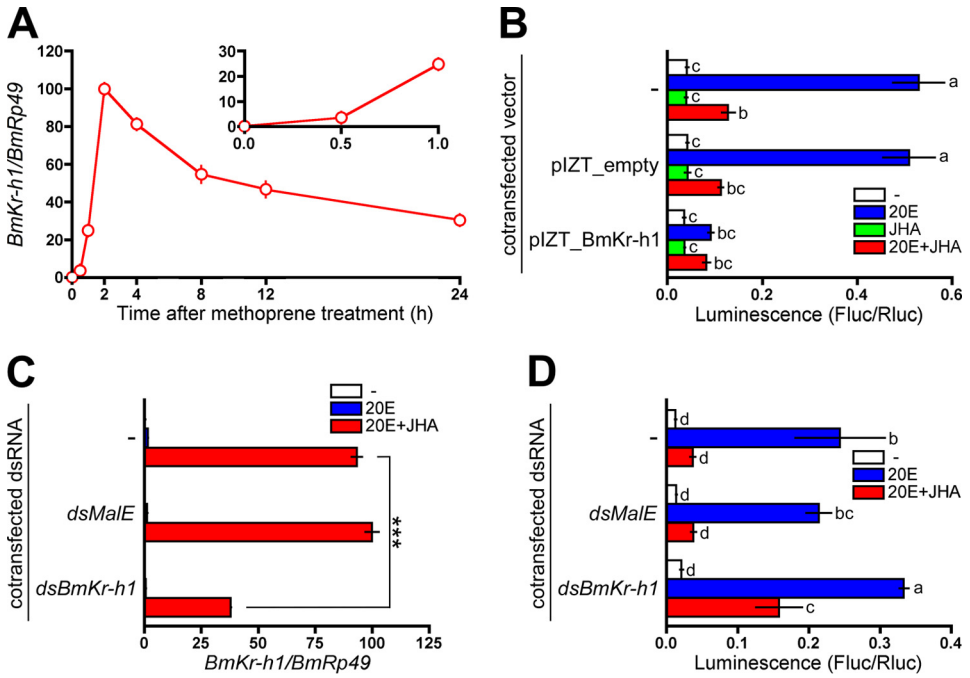

FIGURE 2. **Repression of the *BmBR-C* promoter by BmKr-h1.** *A*, BM-N cells were treated with 10 μM JHA, and temporal changes in *BmKr-h1* expression were monitored by quantitative real-time PCR. *B*, BM-N cells were cotransfected with a reporter plasmid carrying the −5131 to +52 region (pGL4.14), a reference reporter plasmid, and a *BmKr-h1* expression plasmid, and the cells were incubated for 2 days. The transfected cells were treated with 1 μM 20E or 10 μM JHA for 2 days. Reporter activities were measured using a dual-luciferase reporter assay system. *C*, BM-N cells were transfected with *dsBmKr-h1*, and the cells were incubated for 2 days. The transfected cells were treated with 1 μM 20E or 10 μM JHA for 2 days, and the RNAi efficiency was monitored by quantitative real-time PCR. *D*, BM-N cells were cotransfected with a reporter plasmid carrying the −5131 to +52 region (pGL4.14), a reference reporter plasmid, and *dsBmKr-h1*, and the cells were incubated for 2 days. The transfected cells were treated with 1 μM 20E or 10 μM JHA for 2 days. Reporter activities were measured using a dual-luciferase reporter assay system. Data represent the means ± S.D. ($n = 3$). *B* and *D*, *bars* with the same letter are not significantly different (Tukey-Kramer test, $\alpha = 0.05$). *C*, data were analyzed using Student's *t* tests (***, $p < 0.001$).

(ACAAAA and AAAAGGGTTAA) of Krüppel (44, 45) shared no homology with that of KBS core region.

BmKr-h1 Directly Binds to KBS—To demonstrate that BmKr-h1 directly binds to KBS, we performed EMSAs using the KBS sequence (60 bp) as a probe. As shown in Fig. 4*A*, a specific band shift appeared when HA-tagged BmKr-h1 (BmKr-h1_HA) (*lane 3*) was added to the probe and the mixture was incubated for 4 h, whereas only a nonspecific shift was observed when luciferase was added as a mock binding factor (*lane 2*). Competition assays showed that the specific band disappeared upon the addition of 100-fold molar excess of an unlabeled KBS probe (*lane 4*) but not by a nonspecific probe (*lane 5*). This specific band was supershifted by the addition of an anti-HA tag antibody (*lane 6*) but not by an anti-V5 tag antibody (negative control, *lane 7*). These results clearly indicated that BmKr-h1 directly and specifically bound to a DNA sequence in KBS.

Furthermore, we performed EMSAs in which the binding reaction time was shortened from 4 to 2 h to obtain information on the number of BmKr-h1 molecules that interact with the KBS region. Two shifted bands (shift-1 and shift-2) were detected in *lane 3*, which contained BmKr-h1_HA (Fig. 4*B*), suggesting that the shift-1 band was composed of one BmKr-h1 molecule, whereas the shift-2 band was composed of two. Likewise, two shifted bands (shift-3 and shift-4) were observed when incubated with modified BmKr-h1 (BmKr-h1(1–243)) in which the C-terminal region downstream of the zinc finger domains was deleted (Fig. 4*B*, *lane 4*). When BmKr-h1_HA and BmKr-h1(1–243) were mixed, a new shifted band (shift-5) appeared between shift-2 and shift-4, which was diminished by the addition of the specific probe (Fig. 4*B*, *lane 6*) but not by the nonspecific probe (Fig. 4*B*, *lane 7*), suggesting that the shift-5 band was composed of both BmKr-h1_HA and BmKr-h1(1–243) molecules.

Functional Characterization of BmKr-h1—To identify which of the eight zinc finger domains (ZF1–8) in BmKr-h1 is important for binding to the KBS sequence, we constructed eight expression vectors, each lacking one of the eight zinc finger domains. Deletion of ZF2, -3, -7, or -8 resulted in decreases in the reporter activities induced by p65AD-BmKr-h1, whereas no changes in reporter activities were observed when ZF1, -4, -5, or -6 was deleted (Fig. 5*A*). Because potential denaturation of BmKr-h1 protein conformation after deletion of the entire single zinc finger domain was a concern, we instead constructed expression vectors designed to substitute cysteine and histidine, which coordinate Zn^{2+} in the zinc finger domain, with serine and phenylalanine, respectively. Decreased reporter activities were observed when ZF2, -3, -7, or -8 were mutated, which was in complete agreement with the results of the deletion constructs (Fig. 5*B*). C_2H_2 zinc fingers bind to DNA with a specific affinity conferred by several amino acid residues in the α helix of each finger (46). The amino acid residues of the α helix of each zinc finger domain in BmKr-h1 are diverse (9), suggesting that each zinc finger domain of BmKr-h1 recognizes a different sequence in the KBS core region.

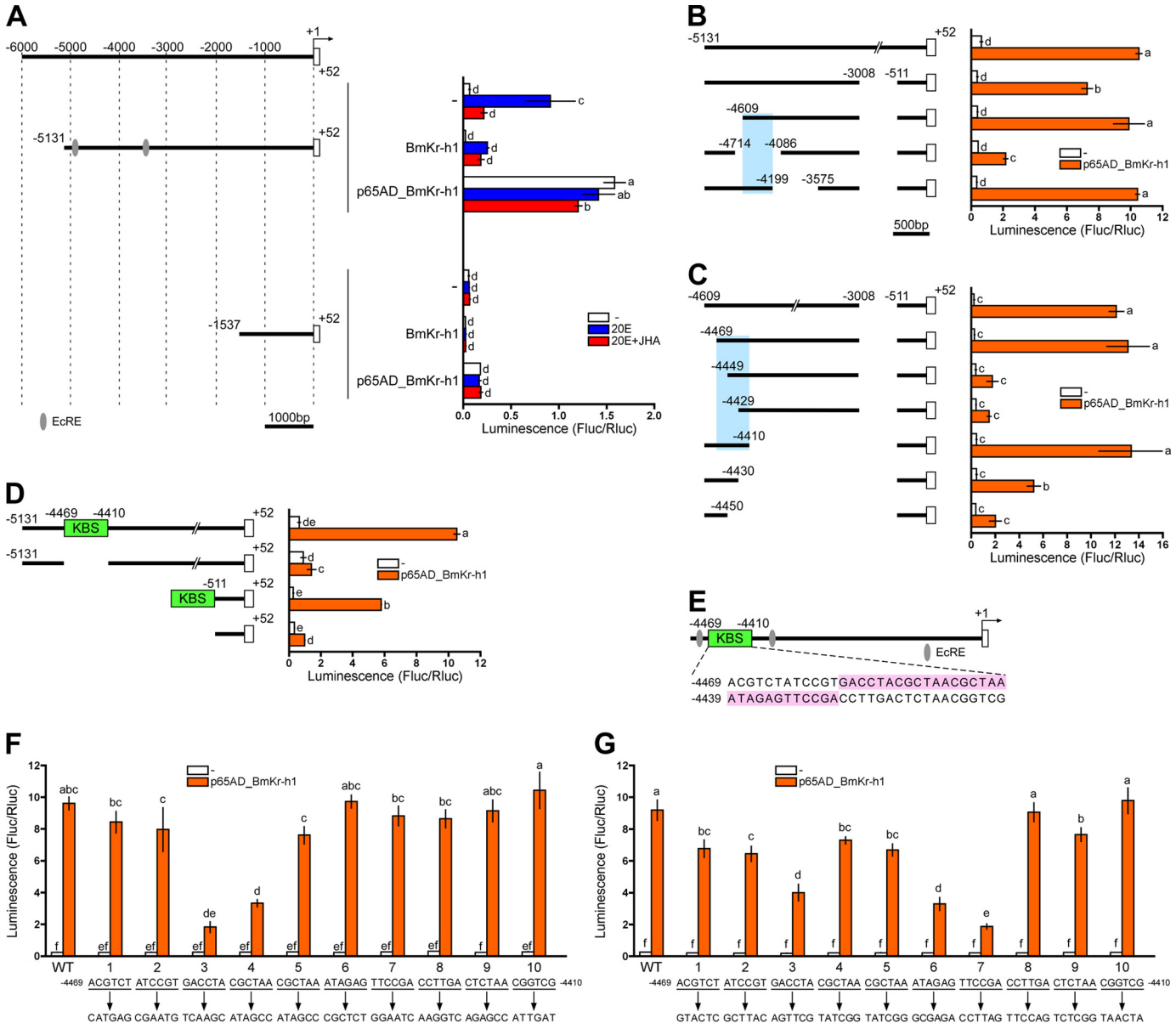

FIGURE 3. **Identification of the BmKr-h1 binding site (*KBS*) in the *BmBR-C* promoter.** Reporter assays using progressive deletion and mutation constructs were performed to identify the KBS region. BM-N cells were cotransfected with pGL4.14 reporter plasmids carrying the promoter regions indicated in the figure, a reference reporter plasmid, and a p65AD-*BmKr-h1* expression plasmid (pIZT). The cells were incubated for 3 days, and reporter activities were measured using a dual-luciferase reporter assay system. Data represent the means ± S.D. ($n = 3$). *Bars with the same letter* are not significantly different (Tukey-Kramer test, $\alpha = 0.05$). *A*, reporter plasmids containing the 5′-flanking regions of *BmBR-C*_P_{dist} (−5131 to +52) and (−1537 to +52) were assayed. *Numbers* indicate the distance from the transcription start site, and *boxes* represent the exons. The cells incubated for 2 days after transfection were treated with 1 μM 20E or 10 μM JHA for 2 days. *B*, reporter activities of progressive deletion constructs are shown below. *Sky blue highlighting* indicates the KBS region. *C*, the *inset* in the plasmid used in *B*, consisting of the −4609 to −3008 and −511 to +52 region, was progressively reduced from both sides by 20 bp, and the effects were measured by reporter assays. *Sky blue highlighting* indicates the region containing KBS. *D*, a reporter carrying the −5131 to +52 region excluding −4469 to −4410 (KBS) and another reporter carrying the KBS region connected to a basal promoter region (−511 to +52) were assayed. *E*, schematic representation of the location of KBS (-4469 to −4410). The nucleotide sequence is shown under the gene structure. *Red ellipses* indicate ecdysone response elements (*EcRE*). The functionality of KBS was assayed with mutations causing a sextuplet transversion (*F*) or transition (*G*) in the KBS (−4469 to −4410) region of the reporter (−4609to −3008 and −511 to +52).

Hormonal Regulation of the BR-C Promoter via Kr-h1 and KBS—Last, we performed a comprehensive analysis of the regulation of *BmBR-C* by 20E and JH via BmKr-h1 and KBS in BM-N cells. The reporter carrying the −5131 to +52 region containing KBS was activated by 20E, and this activation was repressed by JHA (Fig. 6*A*). Ectopic expression of BmKr-h1 repressed the activation of the reporter in the absence of JH (Fig. 6*A*). On the other hand, when KBS was deleted from the reporter carrying −5131 to +52, the repression of reporter activation was not in turn repressed by JH even if BmKr-h1 was ectopically expressed in the cells (Fig. 6*A*). Taking these results together, we propose the following mechanism of the hormonal regulation of *BmBR-C*; in the presence of JH, *BmKr-h1* gene expression is induced by JH via BmMet/Bm-steroid receptor coactivator (9, 12); subsequently, two molecules of BmKr-h1 bind to the KBS sequence of the *BmBR-C* promoter and thereby repress 20E-dependent expression of *BmBR-C* (Fig. 6*B*).

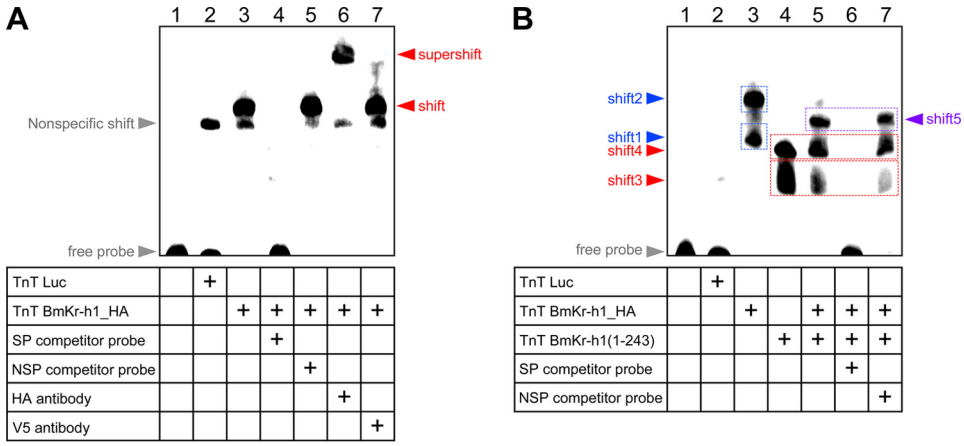

FIGURE 4. **BmKr-h1 directly binds to KBS.** *A* and *B*, EMSA experiments. Luciferase (mock), BmKr-h1-HA, and BmKr-h1(1–243) proteins were synthesized by an *in vitro* transcription and translation system and incubated with a KBS (60 bp) probe labeled with Biotin-ON for 4 h (*A*) or 2 h (*B*). Competition assays were performed using a 100-fold molar excess of unlabeled specific (*SP*) or nonspecific (*NSP*) probes. The specificities of shifted bands were verified using polyclonal antibodies against HA and V5 tags (negative control). Note that the disappearance of shift-3, -4, and -5 by the addition of specific probe (*lane 6*), but not by nonspecific probe (*lane 7*), showed that these all represented specific BmKr-h1 binding.

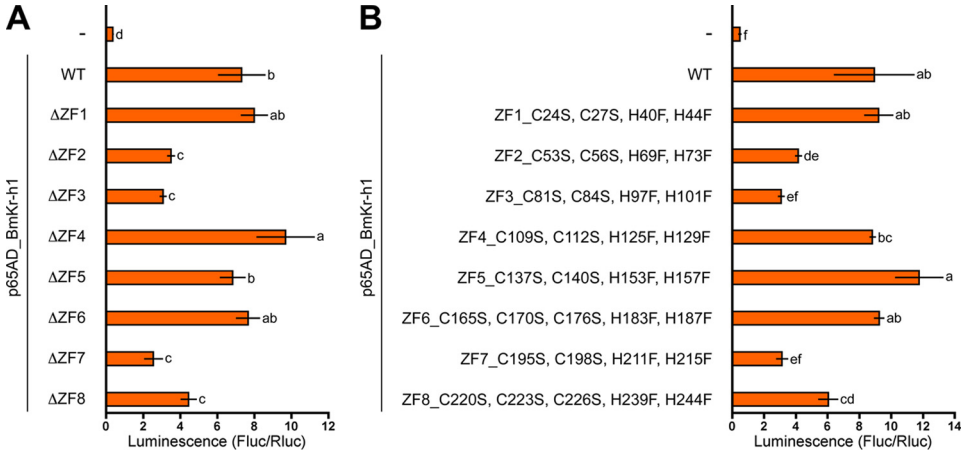

FIGURE 5. **Binding activities of BmKr-h1 mutated in each zinc finger domain.** BM-N cells were cotransfected with a reporter plasmid carrying the −5131 to +52 region (pGL4.14), a reference reporter plasmid, and expression plasmids (pIZT) of p65AD_BmKr-h1 carrying deletions of each zinc finger domain (*A*) or mutated by amino acid substitutions (*B*). The transfected cells were incubated for 3 days, and reporter activities were measured using a dual-luciferase reporter assay system. Data represent the means ± S.D. ($n = 3$). *Bars with the same letter* are not significantly different (Tukey-Kramer test, $\alpha = 0.05$).

The response of *BmBR-C* in BM-N cells to 20E and/or JH is reminiscent of that observed in the larval epidermis and silk gland before pupal commitment (30, 33, 34). At this stage the expression of *BmKr-h1* is maintained at high levels by the continuous presence of JH (20). The decline of JH titer at the beginning of the final instar larvae causes the temporal disappearance of *BmKr-h1* (20). This might facilitate the subsequent induction of *BmBR-C* by 20E after the commitment to the larval-pupal transition (30, 34). Thus, the mechanism proposed above is likely to be applicable within the immature larvae until pupal commitment.

In contrast, the function of BmKr-h1 and KBS in the regulation of *BmBR-C* during metamorphosis seems to be more complex. After pupal commitment, *BmKr-h1* re-expresses at a high level (20) along with *BmBR-C* during the prepupal stage (30). In transgenic silkworms, ectopic expression of *BmKr-h1* did not suppress the induction of *BmBR-C* by 20E in the epidermis of final instar larvae, although the larval-pupal metamorphosis was interrupted (20). Apparently, the BmKr-h1 alone was not sufficient to suppress the expression of *BmBR-C* in the final instar larval stage. Furthermore, exogenous JH induced re-expression of *BR-C* in the epidermis of early pupae in *M. sexta* (28), and *Kr-h1* is involved in the induction of *BR-C* in the pupae of *D. melanogaster* and *Tribolium castaneum* (16, 17). These apparent inconsistencies in the action of Kr-h1 on the regulation of *BR-C* in different developmental stages might result from differences in the cell autonomous factors at each stage, such as the repertoires of transcription factors and co-activator/co-repressors and epigenetic modifications of the promoter as well as the differences in the cell environment including endocrine factors, paracrine factors, and nutrients. Exploration of cofactors involved in the Kr-h1-mediated repression of *BRC* and TALEN-based genome editing of the KBS region would help to gain a unified understanding of the regulation of *BR-C* by *Kr-h1*.

In conclusion, we obtained a comprehensive understanding of the process by which insects avoid precocious entry into metamorphosis. This knowledge would provide important clues to the development of chemicals or treatments that arti-

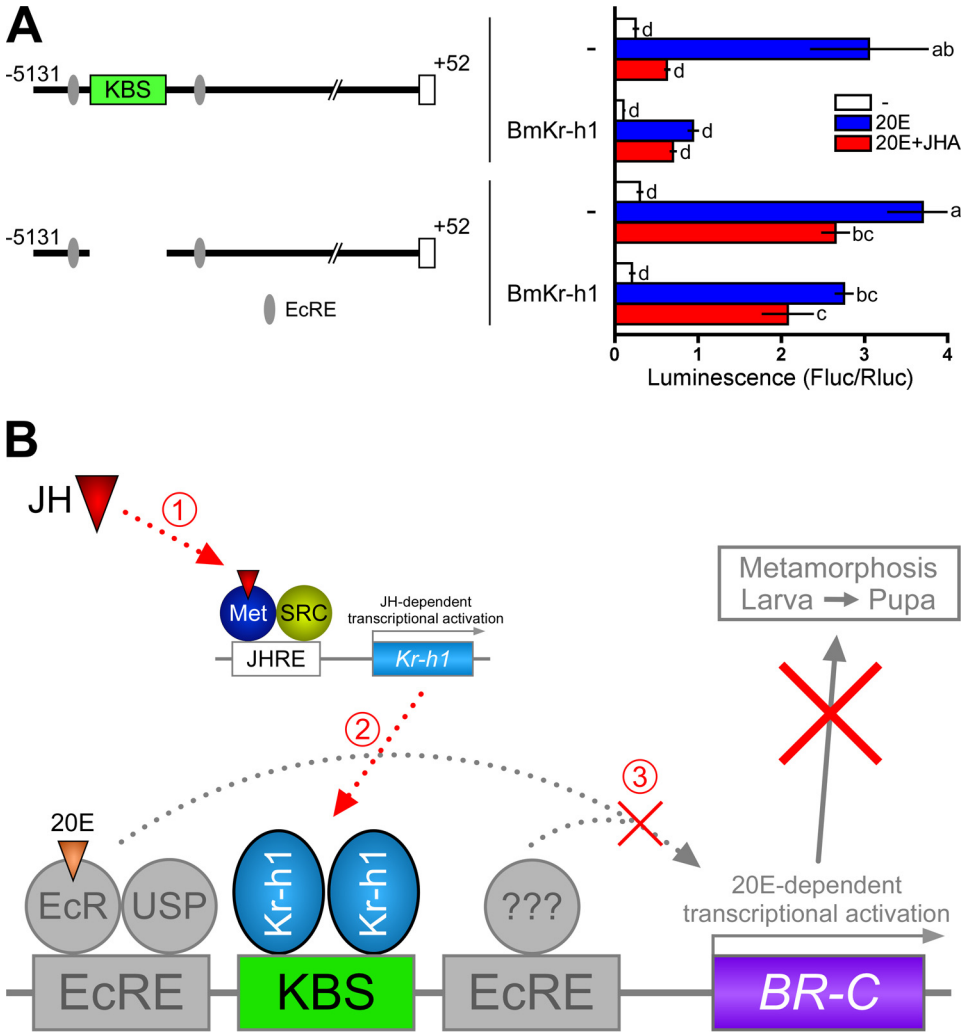

FIGURE 6. **Regulation of the *BR-C* promoter by hormones, Kr-h1, and KBS.** *A*, BM-N cells were cotransfected with a reporter plasmid carrying the −5131 to +52 region without KBS (pGL4.14), a reference reporter plasmid, and a BmKr-h1 expression plasmid, and the transfected cells were incubated for 2 days. The cells were treated with 1 μM 20E or 10 μM JHA for 2 days, and reporter activities were measured by a dual-luciferase reporter assay system. Data represent the means ± S.D. ($n = 3$). *Bars with the same letter* are not significantly different (Tukey-Kramer test, $\alpha = 0.05$). *B*, a model explaining the repression of 20E-dependent induction of *BmBR-C* by JH. *SRC*, steroid receptor coactivator; *EcRe*, ecdysone response element.

ficially facilitate or delay this process, which may be usable in pest management or enhancement of silk production in sericulture.

Author Contributions—T. K., K. N., and Y. N. designed the research. T. K., K. N., Y. Ito, and Y. N. performed the research. T. K., K. N., Y. N., Y. Ishikawa, and T. S. analyzed the data. T. K., Y. Ishikawa, and T. S. wrote the paper.

Acknowledgment—We thank Dr. Toshimasa Yamazaki for helpful advice on protein analysis.

References

1. Riddiford, L. M. (1994) Cellular and molecular actions of juvenile hormone I: general considerations and premetamorphic actions. *Adv. Insect Physiol.* **24,** 213–274
2. Jindra, M., Palli, S. R., and Riddiford, L. M. (2013) The juvenile hormone signaling pathway in insect development. *Annu. Rev. Entomol.* **58,** 181–204
3. Wilson, T. G., and Fabian, J. (1986) A *Drosophila melanogaster* mutant resistant to a chemical analog of juvenile hormone. *Dev. Biol.* **118,** 190–201
4. Ashok, M., Turner, C., and Wilson, T. G. (1998) Insect juvenile hormone resistance gene homology with the bHLH-PAS family of transcriptional regulators. *Proc. Natl. Acad. Sci. U.S.A.* **95,** 2761–2766
5. Miura, K., Oda, M., Makita, S., and Chinzei, Y. (2005) Characterization of the *Drosophila* Methoprene-tolerant gene product. Juvenile hormone binding and ligand-dependent gene regulation. *FEBS J.* **272,** 1169–1178
6. Charles, J. P., Iwema, T., Epa, V. C., Takaki, K., Rynes, J., and Jindra, M. (2011) Ligand-binding properties of a juvenile hormone receptor, Methoprene-tolerant. *Proc. Natl. Acad. Sci. U.S.A.* **108,** 21128–21133
7. Li, M., Mead, E. A., and Zhu, J. (2011) Heterodimer of two bHLH-PAS proteins mediates juvenile hormone-induced gene expression. *Proc. Natl. Acad. Sci. U.S.A.* **108,** 638–643
8. Zhang, Z., Xu, J., Sheng, Z., Sui, Y., and Palli, S. R. (2011) Steroid receptor co-activator is required for juvenile hormone signal transduction through a bHLH-PAS transcription factor, methoprene tolerant. *J. Biol. Chem.* **286,** 8437–8447
9. Kayukawa, T., Minakuchi, C., Namiki, T., Togawa, T., Yoshiyama, M., Kamimura, M., Mita, K., Imanishi, S., Kiuchi, M., Ishikawa, Y., and Shinoda T. (2012) Transcriptional regulation of juvenile hormone-mediated induction of Krüppel homolog 1, a repressor of insect metamorphosis. *Proc. Natl. Acad. Sci. U.S.A.* **109,** 11729–11734
10. Kayukawa, T., Tateishi, K., and Shinoda, T. (2013) Establishment of a

versatile cell line for juvenile hormone signaling analysis in *Tribolium castaneum*. *Sci. Rep.* **3,** 1570
11. Lozano, J., Kayukawa, T., Shinoda, T., and Belles, X. (2014) A role for taiman in insect metamorphosis. *PLoS Genet.* **10,** e1004769
12. Kayukawa, T., and Shinoda, T. (2015) Functional characterization of two paralogous JH receptors, methoprene-tolerant 1 and 2 in the silkworm, *Bombyx mori* (Lepidoptera: Bombycidae). *Appl. Entomol. Zool.* **50,** 383–391
13. Shin, S. W., Zou, Z., Saha, T. T., and Raikhel, A. S. (2012) bHLH-PAS heterodimer of methoprene-tolerant and cycle mediates circadian expression of juvenile hormone-induced mosquito genes. *Proc. Natl. Acad. Sci. U.S.A.* **109,** 16576–16581
14. Cui, Y., Sui, Y., Xu, J., Zhu, F., and Palli, S. R. (2014) Juvenile hormone regulates *Aedes aegypti* Krüppel homolog 1 through a conserved E box motif. *Insect Biochem. Mol. Biol.* **52,** 23–32
15. Li, M., Liu, P., Wiley, J. D., Ojani, R., Bevan, D. R., Li, J., and Zhu, J. (2014) A steroid receptor coactivator acts as the DNA-binding partner of the methoprene-tolerant protein in regulating juvenile hormone response genes. *Mol. Cell. Endocrinol.* **394,** 47–58
16. Minakuchi, C., Zhou, X., and Riddiford, L. M. (2008) *Krüppel homolog* 1 (*Kr-h1*) mediates juvenile hormone action during metamorphosis of *Drosophila melanogaster*. *Mech. Dev.* **125,** 91–105
17. Minakuchi, C., Namiki, T., and Shinoda, T. (2009) *Krüppel homolog* 1, an early juvenile hormone-response gene downstream of *Methoprene-tolerant*, mediates its anti-metamorphic action in the red flour beetle *Tribolium castaneum*. *Dev. Biol.* **325,** 341–350
18. Konopova, B., Smykal, V., and Jindra, M. (2011) Common and distinct roles of juvenile hormone signaling genes in metamorphosis of holometabolous and hemimetabolous insects. *PLoS ONE* **6,** e28728
19. Lozano, J., and Belles, X. (2011) Conserved repressive function of Krüppel homolog 1 on insect metamorphosis in hemimetabolous and holometabolous species. *Sci. Rep.* **1,** 163
20. Kayukawa, T., Murata, M., Kobayashi, I., Muramatsu, D., Okada, C., Uchino, K., Sezutsu, H., Kiuchi, M., Tamura, T., Hiruma, K., Ishikawa Y., and Shinoda T. (2014) Hormonal regulation and developmental role of Krüppel homolog 1, a repressor of metamorphosis, in the silkworm *Bombyx mori*. *Dev. Biol.* **388,** 48–56
21. DiBello, P. R., Withers, D. A., Bayer, C. A., Fristrom, J. W., and Guild, G. M. (1991) The *Drosophila Broad-Complex* encodes a family of related proteins containing zinc fingers. *Genetics* **129,** 385–397
22. Bayer, C. A., Holley, B., and Fristrom, J. W. (1996) A switch in *broad-complex* zinc finger isoform expression is regulated posttranscriptionally during the metamorphosis of *Drosophila* imaginal discs. *Dev. Biol.* **177,** 1–14
23. Spokony, R. F., and Restifo, L. L. (2007) Anciently duplicated *Broad Complex* exons have distinct temporal functions during tissue morphogenesis. *Dev. Genes Evol.* **217,** 499–513
24. Piulachs, M. D., Pagone, V., and Bellés, X. (2010) Key roles of the *Broad-Complex* gene in insect embryogenesis. *Insect Biochem. Mol. Biol.* **40,** 468–475
25. Nagamine, K., Kayukawa, T., Hoshizaki, S., Matsuo, T., Shinoda, T., and Ishikawa, Y. (2014) Cloning, phylogeny, and expression analysis of the Broad-Complex gene in the longicorn beetle *Psacothea hilaris*. *Springerplus* **3,** 539
26. Kiss, I., Bencze, G., Fodor, G., Szabad, J., and Fristrom, J. W. (1976) Prepupal larval mosaics in *Drosophila melanogaster*. *Nature* **262,** 136–138
27. Kiss, I., Beaton, A. H., Tardiff, J., Fristrom, D., and Fristrom, J. W. (1988) Interactions and developmental effects of mutations in the *Broad-Complex* of *Drosophila melanogaster*. *Genetics* **118,** 247–259
28. Zhou, X., and Riddiford, L. M. (2002) Broad specifies pupal development and mediates the "status quo" action of juvenile hormone on the pupal-adult transformation in *Drosophila* and *Manduca*. *Development* **129,** 2259–2269
29. Zhou, X., Zhou, B., Truman, J. W., and Riddiford, L. M. (2004) Overexpression of *broad*: a new insight into its role in the *Drosophila* prothoracic gland cells. *J. Exp. Biol.* **207,** 1151–1161
30. Muramatsu, D., Kinjoh, T., Shinoda, T., and Hiruma, K. (2008) The role of 20-hydroxyecdysone and juvenile hormone in pupal commitment of the epidermis of the silkworm, *Bombyx mori*. *Mech. Dev.* **125,** 411–420
31. Suzuki, Y., Truman, J. W., and Riddiford, L. M. (2008) The role of Broad in the development of *Tribolium castaneum*: implications for the evolution of the holometabolous insect pupa. *Development* **135,** 569–577
32. Konopova, B., and Jindra, M. (2008) Broad-Complex acts downstream of Met in juvenile hormone signaling to coordinate primitive holometabolan metamorphosis. *Development* **135,** 559–568
33. Zhou, B., Hiruma, K., Shinoda, T., and Riddiford, L. M. (1998) Juvenile hormone prevents ecdysteroid-induced expression of broad complex RNAs in the epidermis of the tobacco hornworm, *Manduca sexta*. *Dev. Biol.* **203,** 233–244
34. Reza, A. M., Kanamori, Y., Shinoda, T., Shimura, S., Mita, K., Nakahara, Y., Kiuchi, M., and Kamimura, M. (2004) Hormonal control of a metamorphosis-specific transcriptional factor Broad-Complex in silkworm. *Comp. Biochem. Physiol. B* **139,** 753–761
35. Zhou, B., and Riddiford, L. M. (2001) Hormonal regulation and patterning of the Broad-Complex in the epidermis and wing discs of the tobacco hornworm, *Manduca sexta*. *Dev. Biol.* **231,** 125–137
36. Huang, J., Tian, L., Peng, C., Abdou, M., Wen, D., Wang, Y., Li, S., and Wang, J. (2011) DPP-mediated TGF beta signaling regulates juvenile hormone biosynthesis by activating the expression of juvenile hormone acid methyltransferase. *Development* **138,** 2283–2291
37. Nishita, Y., and Takiya, S. (2004) Structure and expression of the gene encoding a *Broad-Complex* homolog in the silkworm, *Bombyx mori*. *Gene* **339,** 161–172
38. Nishita, Y., and Takiya, S. (2006) Differential usage of two promoters of the *Broad-Complex* gene in the silkworm, *Bombyx mori*. *Insect Biochem. Mol. Biol.* **36,** 779–788
39. Nishita, Y. (2014) Ecdysone response elements in the distal promoter of the *Bombyx Broad-Complex gene, BmBR-C*. *Insect Mol. Biol.* **23,** 341–356
40. Nishita, Y., and Takiya, S. (2009) Differential responsiveness of *BmBR-C* promoters to ecdysone signals. *J. Insect Biotechnol. Sericol.* **78,** 127–138
41. Kobayashi, I., Kojima, K., Uchino, K., Sezutsu, H., Iizuka, T., Tatematsu, K., Yonemura, N., Tanaka, H., Yamakawa, M., Ogura, E., Kamachi Y., and Tamura T. (2011) An efficient binary system for gene expression in the silkworm, *Bombyx mori*, using GAL4 variants. *Arch. Insect Biochem. Physiol.* **76,** 195–210
42. Kanamori, Y., Hayakawa, Y., Matsumoto, H., Yasukochi, Y., Shimura, S., Nakahara, Y., Kiuchi, M., and Kamimura, M. (2010) A eukaryotic (insect) tricistronic mRNA encodes three proteins selected by context-dependent scanning. *J. Biol. Chem.* **285,** 36933–36944
43. Sailsbery, J. K., Atchley, W. R., and Dean, R. A. (2012) Phylogenetic analysis and classification of the fungal bHLH domain. *Mol. Biol. Evol.* **29,** 1301–1318
44. Rosenberg, U. B., Schröder, C., Preiss, A., Kienlin, A., Côté, S., Riede, I., and Jäckle, H. (1986) Structural homology of the product of the *Drosophila Krüppel* gene with *Xenopus* transcription factor IIIA. *Nature* **319,** 336–339
45. Pankratz, M. J., Hoch, M., Seifert, E., and Jäckle, H. (1989) Krüppel requirement for *knirps* enhancement reflects overlapping gap gene activities in the *Drosophila* embryo. *Nature* **341,** 337–340
46. Iuchi, S. (2001) Three classes of C_2H_2 zinc finger proteins. *Cell. Mol. Life Sci.* **58,** 625–635